Fuel Cells DOI: 10.1002/fuce.200800139

Magnetotomography and Electric Currents in a Fuel Cell▲

H. Lustfeld[1]*, M. Reißel[2]*, and B. Steffen[3]*

[1] Forschungszentrum Jülich, IFF, 52425 Jülich, Germany
[2] Fachhochschule Aachen, Campus Jülich, 52428 Jülich, Germany
[3] Forschungszentrum Jülich, JSC, 52425 Jülich, Germany

Received October 31, 2008; accepted June 21, 2009

Abstract

Magnetotomography, applied to fuel cells, gives rise to several questions: first, how well can the electric current density in the fuel cell be reconstructed by measuring its external magnetic field? It is quite clear that the connection between magnetic field and current alone will lead to ambiguous results. Two further relations lead to unique reconstruction: the continuity equation and Ohm's law. Second, application of Ohm's law in the membrane electrode assembly (MEA) of a fuel cell – is it not a questionable procedure? We show that in the MEA Ohm's law is not needed, when applying a rather mild approximation, we call it the 'thin MEA approximation'. The advantage of this is the linear relation between magnetic field and electric current density, not only in the neighbourhood of the operating point but over the whole range. Third, can a functional connection be derived between resolution of the current density and the precision requirements of the measurement devices? We present a procedure leading to a unique relation between the two. This procedure can be extended to finding the optimum measuring positions, thus essentially decreasing the number of measuring points, and thus the time scale of measurable dynamical disturbances, all this without a loss of fine resolution. We present explicit numerical results for two geometries, typical for DMFC and PEMFC fuel cells.

Keywords: Current Density Distribution, DMFC, Fuel Cell, Magnetic Field Measurement, MEA, PEFC, PEMFC, Tomography

1 Introduction

In spite of the fact that fuel cells are now known for more than 150 years [1], their reliability and efficiency are still major problems, and therefore a good diagnostics on the microscopic and the macroscopic scale is very important.

Whereas diagnostics on the microscopic scale cannot be achieved without interfering with the running processes, more or less deeply [2–4], this cannot be said with the same certainty, when looking at properties on a macroscopic scale [5].

One of these macroscopic properties requiring diagnostics is the electric current density in the fuel cell. Here, different kinds of diagnostics are possible [6]. Contacts in segmented [7] or nonsegmented [8] additional layers allow the measuring of these currents. The advantage is the speed at which these measurements can be carried through. As a result, one gets a snapshot of the current density in the fuel cell. Quite different from these procedures, are tomographic methods exploiting the fact that the current density in fuel cells is high [9]. Typical current densities are 0.2 A cm^{-2}, leading to magnetic fields of a size, which is comparable to the earth's magnetic field, namely about 5×10^{-5} T. Thus, it is not surprising that the so called *magnetotomography* was suggested as a tool to reconstruct the current density in a fuel cell by measuring the external magnetic fields. A disadvantage is the time required to measure the external magnetic fields at, sufficiently, many positions. Typical time scales are more of the order of minutes than seconds [10]. Its great advantage is that the method is noninvasive, allowing measurements (i) without influencing the internal processes in a fuel cell, (ii) without extra preparations of the fuel cell. This is why, it is of great interest to investigate the principle applicability of this kind of tomography for realistic parameters and typical dimensions of fuel cells.

▲ *Presented at the 1st CARISMA Conference, Progress MEA 2008, La Grande Motte, France, Oct. 2008*

[*] *Corresponding author, h.lustfeld@fz-juelich.de, reissel@fh-aachen.de, b.steffen@fz-juelich.de*

Two questions have to be answered:

(i) How unique is the information obtained from the external magnetic fields, or more detailed: given a certain relative precision of the measuring devices, how good is the resolution with which the electric current can be determined, in particular the current through the membrane electrode assembly (MEA)?

(ii) At which locations should the magnetic field be measured to obtain optimum tomographic results?

(i) Is the question of invertibility (crucial for any tomographic problem): for each electric current density distribution $\mathbf{j}(\mathbf{r})$ in the fuel cell, the external magnetic field can be computed uniquely – but can $\mathbf{j}(\mathbf{r})$ be uniquely determined from external magnetic field measurements?

A positive answer to this question has been given in part, for several limiting cases [11, 12] but not in generality. The reason for this is easy to recognise by looking at Biot–Savart's law[a] for the magnetic field $\mathbf{H}$.

$$\mathbf{H}(\mathbf{r}) = \frac{1}{4\pi}\int_V d^3r' \frac{\mathbf{j}(\mathbf{r}')\times(\mathbf{r}-\mathbf{r}')}{|\mathbf{r}-\mathbf{r}'|^3} \tag{1}$$

By inspecting this formula, it becomes quite clear that one has to know the current density $\mathbf{j}(\mathbf{r})$ at many locations in the whole fuel cell to determine the external magnetic field. This means that for the inverse problem, the number of locations becomes huge at which $\mathbf{j}(\mathbf{r})$ is unknown and has to be determined from the external data. So, it is rather obvious that the inverse problem cannot be solved without exploiting further restrictions [9]. One of these restrictions is the continuity equation.[b]

$$\nabla\mathbf{j}(\mathbf{r}) = 0 \tag{2}$$

But this is not enough for getting a unique inverse problem. Another restriction is due to a functional relation between $\mathbf{j}(\mathbf{r})$ and the electric field $\mathbf{E}(\mathbf{r})$. In conductors (metals, graphite, etc.), these quantities are connected in a very simple way, by Ohm's law.

$$\mathbf{j}(\mathbf{r}) = \sigma(\mathbf{r})\mathbf{E}(\mathbf{r}) \tag{3}$$

Here, σ is the specific conductivity. In contrast to conductors, however, the relation between current and electric field is not at all that simple in the MEA of a fuel cell, since the electric currents in the MEA are due to complicated physical and chemical processes [13]. A way out of this dilemma consists of looking at deviations from the operating point. With $\mathbf{j}_{op}(\mathbf{r})$ and $\mathbf{E}_{op}(\mathbf{r})$ describing $\mathbf{j}$ and $\mathbf{E}$ at the operating point we get for the deviations from the operating point in linear approximation.

$$\mathbf{j}(\mathbf{r}) - \mathbf{j}_{op}(\mathbf{r}) = \sigma(\mathbf{r})\Big[\mathbf{E}(\mathbf{r}) - \mathbf{E}_{op}(\mathbf{r})\Big] \tag{4}$$

It has been shown that by using Eq. (4), the inverse problem becomes unique [14] for calculating deviations from the operating point – at least up to a certain resolution, provided that the deviations from the operating point are not too large.

Nevertheless, Eq. (4) is unsatisfactory. It is not only a linear approximation but the operating point itself depends on the dynamical state of the fuel cell. Therefore, it is difficult to get results about the absolute currents and fields.

It is the aim of the present paper to show that one can do without Eq. (4). We will show in Section 2, that this is possible because the thickness of the MEA and in particular that of the electrolyte in the MEA is small. Since Eq. (4) is not needed anymore, the actual values of the electric current density $\mathbf{j}(\mathbf{r})$ and the electric fields $\mathbf{E}(\mathbf{r})$ can be calculated without referring to the operating point. In Section 3, we apply the formulas developed in Section 2. In particular, the connection between relative precision of a measuring device and resolution obtainable for $\mathbf{j}$ is presented for two (representative) cases: (i) for an experimental DMFC being used in the Forschungszentrum Jülich (FZJ), (ii) a PEMFC with a geometry used in the Zentrum für Brennstoffzellen Technologie (ZBT) in Duisburg. The main result of Section 3 is the message that the magnetotomography is applicable if (i) a relative precision of the devices measuring the magnetic fields can be guaranteed to be $\approx 10^{-4}$, (ii) one is content with a resolution of ≈1 cm for fuel cells having the dimensions of the experimental DMFC in the FZJ and of ≈0.5–1 cm for fuel cells having the dimensions of the experimental PEMFC of the ZBT. In Section 4, we deal with the problem of optimising the measuring points, i.e. how the number of measuring points can be reduced essentially *leaving the results qualitatively and quantitatively unchanged, or in other words, without loss of relative precision*. Already, from the point of view that magnetic field measurements are time consuming this is an important topic. Since this has already been described [14–16], we can be rather short here. The conclusion ends the paper.

2 Electric Current Density in the MEA and the External Magnetic Field

Ohm's law Eq. (3) is valid in the bipolar plates and in the metallic layers, etc. with conductivities σ depending, in a very good approximation, on the material only and *via* that on the position $\mathbf{r}$. This is quite different in the MEA. The relation between current and voltage drop in the MEA does not follow Ohm's law. The chemical processes of catalysis at anode and cathode as well as the migration of ions through the electrolyte are not at all processes connecting voltage drop and current in a linear manner. Of course, we can plot local char-

[a] *This formula is valid as long as external perturbation fields can be neglected and the time dependence of all fields is negligible. The formula also holds true if static external perturbations are present but only magnetic field differences between two situations are of interest.*

[b] *Throughout this paper it has been used that for our purposes time dependencies in Maxwell's equations need not be taken into account.*

acteristics. Let us define by $\mathbf{r}_{S_A}$, a point on the surface S_A of the MEA at the side of the anode, and by $\mathbf{r}_{S_C}$, the equivalent point on the surface S_C of the MEA at the side of the cathode, cf. Figure 1. Furthermore let $j_n(\mathbf{r}_{S_A})$ be the current flowing into the MEA at $\mathbf{r}_{S_A}$. Plotting the voltage drop Φ at the MEA against $j_n(\mathbf{r}_{S_A})$, we can formally write.

$$j_n(\mathbf{r}_{S_A}) = \sigma_{\text{drop}}(\mathbf{r}_{S_A}) \frac{\Phi(\mathbf{r}_{S_C}) - \Phi(\mathbf{r}_{S_A})}{d_{\text{MEA}}} \quad (5)$$

Here, d_{MEA} is the thickness of the MEA, and therefore σ_{drop} has the dimension of a specific conductivity. However, it does not depend only on the position but on the voltage and the dynamical status of the MEA as well. This shows that σ_{drop} is a very complicated quantity, difficult to calculate something, with, and without clear physical interpretation. In spite of the obscurity of Eq. (5), $j_n(\mathbf{r}_{S_A})$ is an interesting quantity. First, we observe that $j_n(\mathbf{r}_{S_A})$ has a clear physical meaning and reflects the state of the MEA. Second, the vast majority of the ions migrate through the electrolyte, choosing the shortest way as a consequence of the relative immobility of the ions in the electrolyte and the small cross-section available for transverse currents. The situation is similar at the catalysts of anode and cathode. Therefore, in this regime, the *transverse* electric conductivity is expected to be small, since physico-chemical processes determine the conductivity. Thus, we can state that to a very good approximation the normal component of the current entering this regime at $\mathbf{r}_{S_A}(\mathbf{r}_{S_C})$ of the surface will pass through and will leave the MEA at the equivalent position[c] $\mathbf{r}_{S_C}(\mathbf{r}_{S_A})$. Third, we can now avoid the spurious conductivities in the MEA by setting.

$$j_n(\mathbf{r}_{S_A}) = j_n(\mathbf{r}_{S_C}) \text{ for all } \mathbf{r}_{S_A} \quad (6)$$

This equation will be fulfilled best if the MEA is thin, so we call it the *thin MEA approximation*. Because of its physical importance we define.

$$j_{\text{MEA}}(\mathbf{r}_{S_A}) = j_n(\mathbf{r}_{S_A}) \quad (7)$$

Then, the forward problem of magnetotomography consists of calculating the external magnetic fields for a given j_{MEA}. We achieve this in two steps.

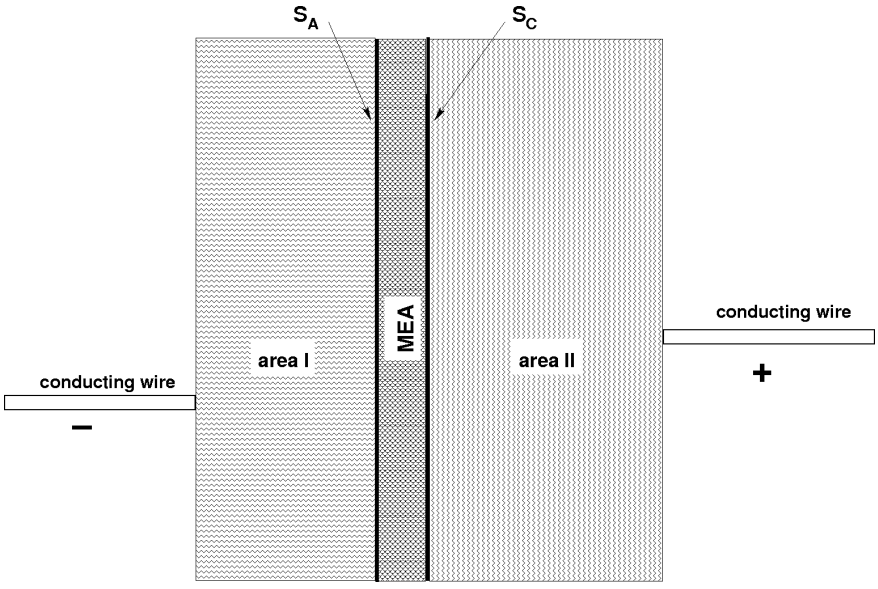

Fig. 1 Scheme of an experimental fuel cell of the DMFC or PEMFC type, respectively. The heart of the cell is the MEA layer limited by the two surfaces S_A and S_C. The current flows through the conduction wires. The MEA divides the fuel cell into area *I* and area *II*. Both areas consist of materials with well-defined specific conductivity, e.g. graphite, stainless nonmagnetic steel, etc.

(A) The current density $\mathbf{j}(\mathbf{r})$ in the fuel cell is computed. To do this, the equation

$$\nabla \mathbf{j} = 0 \quad (8)$$

has to be solved. We choose the j_n current density on the surface S_A as parameter and conclude from Eq. (6) that the problem can be divided into two areas, cf. Figure 1.

(I) The surface of area *I* consists of three parts: (i) S_a is the transverse section of the conduction wire where it touches the fuel cell, (ii) S_A is the surface of the MEA on the side of the anode, (iii) S_{F_I} presents the surface of area *I* of the fuel cell -S_A and S_a. With *J* being the total current, we obtain the following boundary conditions in area *I*:

$$\begin{aligned} &j_n = -J/|S_a| \text{ for } \mathbf{r} \in S_a \\ &j_n = j_{\text{MEA}}(\mathbf{r}_{S_A}) \text{ for } \mathbf{r} \in S_A \\ &j_n = 0 \text{ for } \mathbf{r} \in S_{F_I} \\ &J = \int_{S_A} \mathrm{d}f \, j_{\text{MEA}}(\mathbf{r}) \end{aligned} \quad (9)$$

Since in area *I* there are well defined conductors, we may use Ohm's law, Eq. (3). Moreover, an electric potential, Φ_I, exists, fulfilling.

$$\mathbf{E} = -\nabla \Phi_I \quad (10)$$

Combining equations Eqs. (8)–(10), we obtain

$$\nabla(\sigma \nabla \Phi_I) = 0 \quad (11)$$

[c] *Of course there may exist layers, still within the MEA but outside the regime of electrolyte and catalysts, having a possibly non negligible transverse conductivity. For simplicity we exclude this possibility. If required, there is no reason not to take these layers into account, because there the conductivity is again a property of the material.*

with

$$\begin{aligned} -\sigma\frac{\partial\Phi_I}{\partial n} &= -J/|S_a| \text{ for } \mathbf{r}\in S_a \\ -\sigma\frac{\partial\Phi_I}{\partial n} &= j_{MEA}(\mathbf{r}) \text{ for } \mathbf{r}\in S_A \\ \frac{\partial\Phi_I}{\partial n} &= 0 \text{ for } \mathbf{r}\in S_{F_I} \end{aligned} \tag{12}$$

Φ_I is uniquely determined up to a constant[d] by Eqs. (11) and (12).

(II) In area *II*, the surface is again a union of three surfaces (i) S_c is the transverse section of the second conduction wire where it touches the fuel cell, (ii) S_C is the surface of the MEA on the side of the cathode, (iii) $S_{F_{II}}$ presents the surface of area *II* of the fuel cell minus S_C and S_c. With *J* being the total current, we obtain the following boundary conditions in area *II*:

$$\begin{aligned} -\sigma\frac{\partial\Phi_{II}}{\partial n} &= J/|S_c| \text{ for } S_c \\ -\sigma\frac{\partial\Phi_{II}}{\partial n} &= -j_{MEA}(\mathbf{r}_{S_A}) \text{ for } S_C \\ \frac{\partial\Phi_{II}}{\partial n} &= 0 \text{ for } S_{F_{II}} \end{aligned} \tag{13}$$

Φ_{II} is uniquely determined up to a constant by Eqs. (11) and (13).

With the computations of Φ_I and Φ_{II} the current density, $\mathbf{j}(\mathbf{r})$, can be calculated in the fuel cell except in the MEA where we set on each straight line connecting $\mathbf{r}_{S_A}$ with $\mathbf{r}_{S_C}$

$$\mathbf{j}(\mathbf{r}) = \mathbf{n}(\mathbf{r}_{S_A})j_{MEA}(\mathbf{r}_{S_A}) \tag{14}$$

where $\mathbf{n}$ is the normal vector, directed into the MEA. This formula is consistent with Eq. (6).

(B) After obtaining the current density, $\mathbf{j}(\mathbf{r})$, in the fuel cell, the magnetic field can be calculated from Maxwell's equations. Assuming the absence of external disturbances, we can use the law of Biot–Savart [(Eq. (1)] and obtain the magnetic field $\mathbf{H}$ induced by j_{MEA}.

It is important to realise that the relation between the external magnetic field and j_{MEA} is linear. In fact, if $j^{(1)}_{MEA}$ leads to the external magnetic field $\mathbf{H}_1$ and $j^{(2)}_{MEA}$ to $\mathbf{H}_2$, then each linear combination

$$j^{(t)}_{MEA} = \alpha j^{(1)}_{MEA} + \beta j^{(2)}_{MEA} \tag{15}$$

leads to the magnetic field

$$\mathbf{H}_t = \alpha\mathbf{H}_1 + \beta\mathbf{H}_2 \tag{16}$$

Thus, we can write

$$\mathbf{H} = \tilde{S}j_{MEA} \tag{17}$$

where $\tilde{S}$ is a linear operator to be determined in the forward problem of tomography. This will be done in Section 3. The inverse problem consists of finding out the restrictions under which the inverse Operator $\tilde{S}^{-1}$ exists. This will be discussed in Section 3 and 4.

The procedure described here has the advantage of being linear and avoiding the introduction of artificial conductivities. It contains one arbitrariness: The voltage drop in the MEA is given by $\Phi_I(\mathbf{r}_{S_C}) - \Phi_{II}(\mathbf{r}_{S_A})$. But neither currents nor magnetic fields are changed when adding a term $C(J)$, that does not depend on $\mathbf{r}$, to either Φ_I or Φ_{II}. Therefore, it is not possible to get the characteristics, i.e. the plot *J versus* voltage[e] drop of the cell.

3 Numerical Results: Achievable Resolution in the MEA and Required Precision

The numerical task consists of approximating the operator $\tilde{S}$ in Eq. (17) by a matrix *S*. As described in Section 2, this is done in two steps. First, the partial differential equation, Eq. (11) is solved numerically for the two areas *I* and *II*, cf. Figure 1. We use the finite volume method [17], which is a grid method. The grid spacing along the axis of the fuel cell is, of course, small, namely a fraction of the various layer thicknesses. On the other hand, the transverse grid spacing fixes the resolution of j_{MEA} on the MEA surface, S_A, in a very natural way.

The number of grid points, N_g, on the surface S_A, determines the number of columns[f], N_c, in *S*

$$N_c = N_g - 1 \tag{18}$$

After computing the current densities in areas *I* and *II* by the finite volume method, the external magnetic field $\mathbf{H}$ is obtained using Biot–Savart's law, Eq. (1). If the number of measuring points is $N_{\mathbf{H}}$, then the number of rows in *S* is $3N_{\mathbf{H}}$.

Starting with an orthonormal basis for the discrete approximate of j_{MEA} on S_A, we applied the above scheme by calculating the corresponding magnetic field components of each measuring point for each vector of the orthonormal basis. From this, we got the $3N_{\mathbf{H}} \times N_c$ matrix *S*, which is the best representation of the operator *S* for the chosen resolution and the chosen measuring points.

The properties of matrices can be extracted from a singular value decomposition:

[d] *up to a constant means up to a term not depending on r.*

[e] *It should be mentioned that this arbitrariness is not an artifact of the present procedure but intrinsic: Knowledge of electric currents does not give unique information about voltages. This holds true even in simple circuits. The arbitrariness mentioned is removed if the total voltage drop of the cell is known as function of J.*

[f] *Because of the restriction for j_{MEA} in Eq. (9) the number of free parameters of this quantity is reduced by 1.*

$$
\begin{aligned}
S &= U_S W_S V_S^T \\
U_S &= 3N_{\mathbf{H}} \times N_c \text{ orthogonal matrix} \\
W_S &= N_c \times N_c \text{ diagonal matrix and} \\
& \quad W_{Si,i} \geq W_{Si+1,i+1} \geq 0 \\
V_S &= N_c \times N_c \text{ unitary matrix}
\end{aligned}
\tag{19}
$$

The rank of S is determined by the rank of W_S. In all our computations, we found that the rank was N_c. It means that the inverse problem is always solvable and that magnetotomography always works – in principle, i.e. if the devices could measure the magnetic fields exactly. However, in real life, the precision of devices is limited by a relative error Δ_{rel}. This is harmless if the condition number, n_{con}, of the matrix is not too high, more precisely.

$$\Delta_{rel} < \frac{1}{n_{con}} \tag{20}$$

The condition number is directly given by the singular value decomposition through

$$\frac{1}{n_{con}} = \frac{W_{S N_c,N_c}}{W_{S 1,1}} \tag{21}$$

In this way, we have a relation between resolution and relative precision, the measuring devices have to comply with to guarantee that resolution. For two examples being typical for DMFC and PEMFC fuel cells (cf. Figures 2 and 3), results are shown in Figure 4.

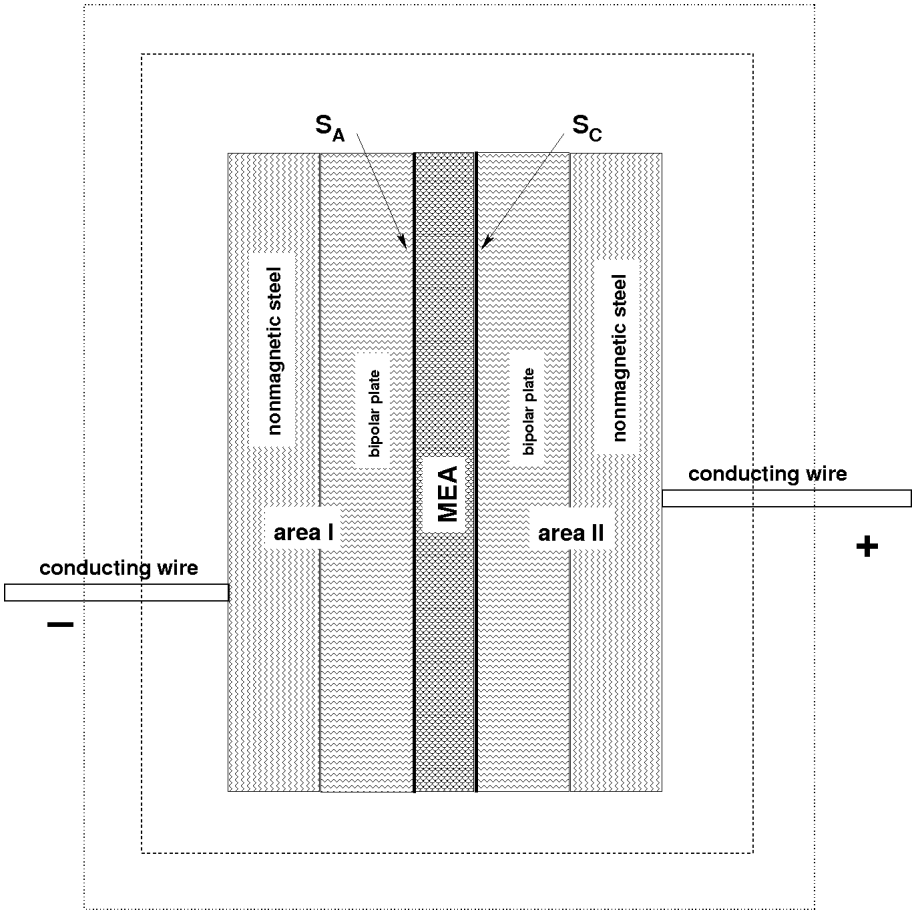

Fig. 2 Dimensions of a fuel cell, used in this paper, with nearly quadratic transverse section. Dimensions are similar to fuel cells investigated in the FZJ, Jülich (Germany): dimensions of MEA, 0.6 mm × 13.8 cm × 17.8 cm; dimensions of flowfield in bipolar plates, 2.0 mm × 13.8 cm × 17.8 cm; dimensions of steel plates, 2.0 mm × 13.8 cm × 17.8 cm. The exterior dimensions (indicated by dashed lines) of the fuel cell are 8.6 mm × 15.8 cm × 24.0 cm. The measuring points of the magnetic field are located on six planes (indicated by dotted lines) around the fuel cell in a distance of 1 cm from the fuel cell.

Typical achievable absolute precisions are of the order[g] of 10^{-8} T, relative precisions of the order of 10^{-4}. Typical strength of the magnetic fields is about 10^{-5} T. This means the following

- type I (used for example in the FZJ): the resolution of magnetotomography reaches its limit at about 1 cm. Better resolutions would require highly sophisticated measuring devices and nearly complete screening of magnetic fields from external sources.
- type II (used for example in the ZBT): the resolution of magnetotomography reaches its limit at about 0.5–1 cm. In analogy to type I, a better resolution would require highly sophisticated measuring devices and nearly complete screening of magnetic fields from external sources.

4 Reduction of the Number of Measuring Points

In the last section, the measuring points were distributed in equal distances over the six planes around the fuel cells. The number of measuring points distributed in this way is large, each measurement is time consuming and therefore dynamical changes in the electric current density are not easily detected if they occur on a small timescale. Thus, the

[g] *Flashlights fabricated from plastics can, when switched on, generate fields on the order of 10^{-8} T in the immediate neighborhood, about 0.3m. The same holds true for power supply units of electronic devices generating high dc currents (50A or more), if inserted in a cheap steel box. Then the screening will be strong enough to reduce the generated perturbation fields to 10^{-8} T or less at a distance of 0.5 m. Moreover standdard measuring devices can contain a low-pass filter with a cutoff frequency of ≈20 Hz. Therefore we think that measurements of magnetic fields of the order of 10^{-8} T can successfully be carried through.*

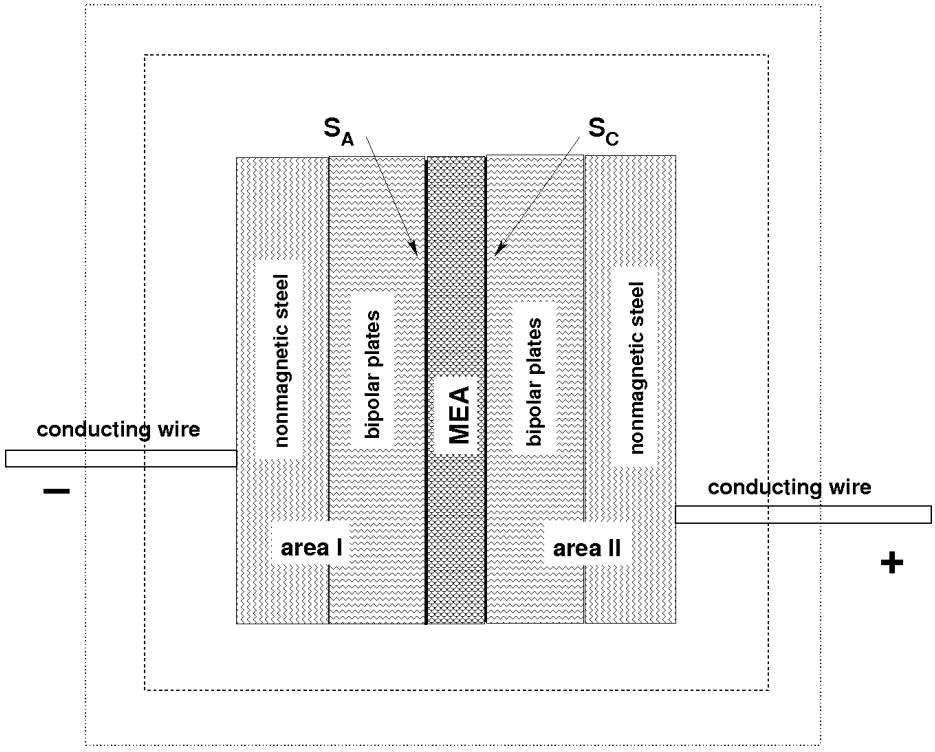

Fig. 3 Dimensions of a fuel cell used in this paper with strong deviations from quadratic transverse section. Dimensions are similar to fuel cells investigated in the ZBT, Duisburg (Germany): dimensions of MEA, 0.6 mm × 9.5 cm × 5 cm; dimensions of flowfield in bipolar plates, 2.0 mm × 9.5 cm × 5 cm; dimensions of steel plates, 2.0 mm × 9.5 cm × 5 cm. The exterior dimensions (indicated by dashed lines) of the fuel cell are 8.6 mm × 14.0 cm × 6.2 cm. The measuring points of the magnetic field are located on six planes (indicated by dotted lines) around the fuel cell at a distance of 1 cm from the fuel cell.

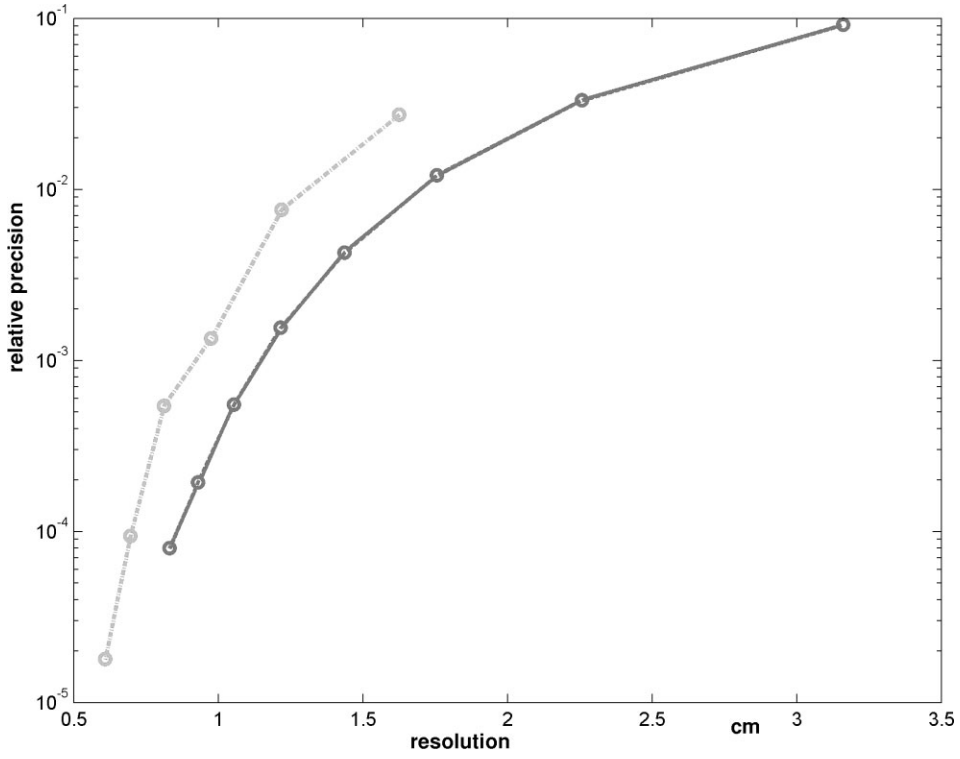

Fig. 4 resolution of **j(r)** in the MEA *versus* logarithm of the required relative precision, when measuring the magnetic field. Distance between the fuel cell and the planes in which the magnetic field is measured is 1 cm. The spacing between the measuring points on the planes is 0.5 cm in longitudinal and 1 cm in lateral direction. (Red) solid line: results for a fuel cell with nearly quadratic transverse section, cf Figrue 2. (Green) dashed dotted line: results for a fuel cell with nonquadratic transverse section, cf. Figure 3.

question arises whether all these measuring points are really necessary. At first glance, one would perhaps think that a measuring point is less important the smaller the magnetic field is at that point. But that need not be true at all. The magnetic field at that point may contain a lot of information about high resolution components of j_{MEA} on S_{A}. On the other hand, there are measuring points bearing nearly no relevant information but magnifying small errors of the measurement. Removal of those points will increase, not decrease the relative precision.

Clearly, a measure of relevance is needed giving a criterion which measuring points are dispensable or should even be removed anyway. Such a measure is the ζ function, which has been introduced and discussed comprehensively in ref. [14–16]. It is defined as

$$\zeta\left(\mathbf{r}_j\right) = \frac{N_{\mathbf{H}}}{N_{\mathrm{c}}} \sum_{m=0}^{2} \left(U_S U_S^T\right)_{3j+m,3j+m} \tag{22}$$

Here $\mathbf{r}_j$ is the position of a measuring point and U_S has been defined in Eq. (19). The ζ function has the property

$$\frac{1}{N_{\mathbf{H}}} \sum_{i=1}^{N_{\mathrm{H}}} \zeta(\mathbf{r}_i) = 1 \tag{23}$$

ζ can be used as criterion for finding the relevant set from $N_{\mathbf{H}}$ measuring points: let d_ζ be a constant having been fixed in the beginning. Then we select the relevant measuring positions $\mathbf{r}_j$ according to:

$$\text{if } \zeta\left(\mathbf{r}_j\right) \geq d_\zeta, \text{ then the measuring point at } \mathbf{r}_j \text{ is kept} \tag{24}$$

d_ζ does not have to be small. A typical value is 2, i.e. twice the average of ζ.

Results are presented in Figures 5–7. It is surprising to note the extent to which the number of measuring points can be reduced *without loosing relative precision. In other words, the results remain qualitatively and quantitatively the same – or become even better*. It should be pointed out that the remaining points represent the best choice in the sense that their selection does not depend on the strength or kind of the perturbation. In all cases, their choice leads to results as good as the original arrangement of the measuring points – or even better ones.

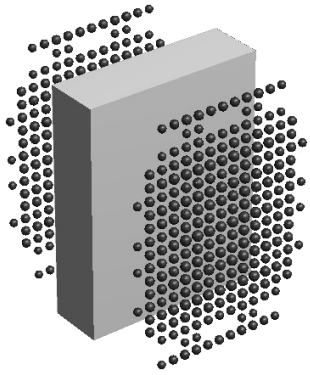

Fig. 5 For a fuel cell with nearly quadratic transverse section (cf. Figure 2), the remaining 458 measuring points (lying on only two surfaces) out of the original 1466 (lying on six surfaces) are shown. The other points have been discarded according to the ζ function criterion. Spacing between the measuring points is originally about 0.5 cm in longitudinal and 1 cm in lateral direction. At each measuring point, the value of the ζ function is indicated by the thickness of the corresponding marker. Note that the scales in depth, width and height are not identical.

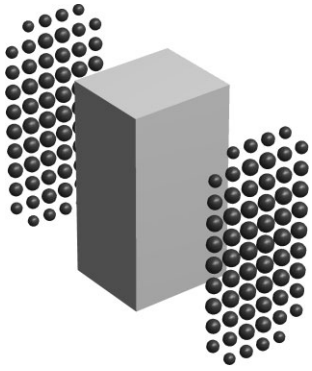

Fig. 6 For a fuel cell with non-quadratic transverse section (cf. Figure 3) the remaining 124 measuring points (lying on only two surfaces) out of the original 570 (lying on six surfaces) are shown. The other points, have been discarded according to the ζ function criterion. Spacing between measuring points is originally about 0.5 cm in longitudinal and 1 cm in lateral direction. At each measuring point the value of the ζ function is indicated by the thickness of the corresponding marker. Note that the scales in depth, width and height are not identical.

5 Conclusion

In this paper, we have numerically investigated the application of magnetotomography on typical fuel cells like DMFC and PEMFC. Whereas magnetic field measurements alone lead only to ambiguous information about the electric currents in the fuel cell, the extensive use of the continuity equation and Ohm's law makes this problem uniquely solvable at reasonable resolutions.

Due to a (mild) approximation (the thin MEA approximation), we need not rely on Ohm's law in the MEA of the fuel cells where Ohm's law is rather questionable indeed. As a consequence we can get information about the electric current density far away from the operating point also.

It turns out that the currents passing through the MEA can be determined with a resolution in the order of 1 cm if a relative precision of devices, measuring the external magnetic field, can be maintained at 10^{-4}.

We have shown that the number of measuring points, determining the external magnetic field, can be reduced by 80% without loss of relative precision offering the chance of measuring dynamical processes with this method.

Numerical calculations for fuel cell stacks are in progress. Due to the fact that for inner cells of a stack, the measuring positions, that are most important for a single cell, are not available, the resolution is expected to be much less; exactly how much, remains to be seen.

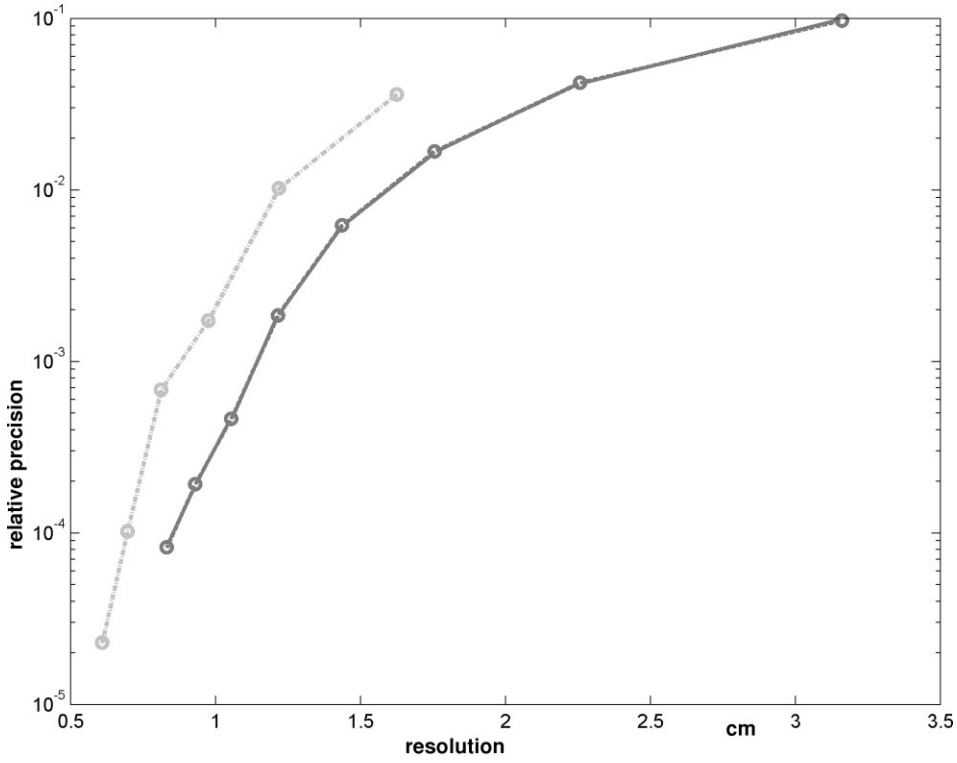

Fig. 7 Resolution of **j**(**r**) in the MEA *versus* logarithm of the required relative precision, when measuring the magnetic field. In contrast to Figure 4, only those measuring points having passed the ζ function criterion are taken into account. Distance between the fuel cell and the planes in which the magnetic field is measured is 1 cm. (Red) solid line: results for a fuel cell with nearly quadratic transverse section, cf. Figure 2. (Green) dashed dotted line: results for a fuel cell with nonquadratic transverse section, cf. Figure 3. There is obviously nearly no difference between the plots here and those of Figure 4. The results are even slightly better showing the efficiency of the reduction procedure.

Moreover, experiments are under way to further investigate the possibilities of magnetotomography and to validate our numerical results.

Acknowledgements

We would like to thank J. Hirschfeld for stimulating discussions.

References

[1] A. J. Appleby, F. R. Foulkes, "*Fuel Cell Handbook*", van Nostrand Reinhold, New York, 1988.
[2] B. Mecheri, A. D'Epifanio, E. Traversa, S. Licoccia, *J. Power Sources* **2008**, *178*, 554.
[3] J. S. Paddison, *Annu. Rev. Mater. Res.* **2003**, 289.
[4] G. Gebel, O. Diat, *Fuel Cells* **2005**, *5*, 261.
[5] K.-H. Hauer, R. Potthast, T. Wüster, D. Stolten, *J. Power Sources* **2005**, *143*, 67.
[6] M. Wilkinson, M. Blanco, E. Gu, J. J. Martin, D. P. Wilkinson, J. J. Zhang, H. Wang, *Electrochem. Solid-State Lett.* **2006**, *9*, A507.
[7] A. Hakenjos, H. Muenter, U. Wittstadt, C. Hebling, *J. Power Sources* **2004**, *131*, 213.
[8] R. Eckl, R. Grinzinger, W. Lehnert, *J. Power Sources* **2006**, *1543*, 171.
[9] R. Kress, L. Kühn, R. Potthast, *Inverse Probl.* **2002**, *18*, 1127.
[10] D. U. Sauer, T. Sanders, B. Fricke, T. Baumhöfer, K. Wippermann, A. A. Kulikovsky, H. Schmitz, J. Mergel, *J. Power Sources* **2008**, *176*, 477.
[11] R. Potthast, L. Kühn, *Math. Methods Appl. Sci.* **2003**, *26*, 739.
[12] K.-H. Hauer, R. Potthast, M. Wannert, *Inverse Probl.* **2008**, *24*, 045008.
[13] P. Debye, *Trans. electrochem. Soc.* **1942**, *82*, 265.
[14] H. Lustfeld, M. Reißel, U. Schmidt, B. Steffen, *J. Fuel Cell Sci. Technol.* **2009**, *6*, 021012.
[15] more detailed results are presented in: U. Schmidt, "Numerische Sensitivitätsanalyse für ein Tomographieproblem bei Brennstoffzellen", *Diploma Thesis*, Fachhochschule Aachen, Abteilung Jülich, Jülich, **2007**.
[16] more detailed results are presented in: R. Telschow, "Untersuchungen zur Reduktion des Messaufwandes bei der Magnetotomographie von Brennstoffzellen", *Diploma Thesis*, Fachhochschule Aachen, Abteilung Jülich, Jülich 2008.
[17] E. Haber, U. M. Ascher, *Siam J. Sci. Comput.* **2001**, *22*, 1943.

